

Article

# Degradation of Polypropylene Membranes Applied in Membrane Distillation Crystallizer

Marek Gryta

Institute of Inorganic Technology and Environment Engineering, West Pomeranian University of Technology, Szczecin, ul. Pułaskiego 10, 70-322 Szczecin, Poland; marek.gryta@zut.edu.pl; Tel.: +48-91-449-47-30; Fax: +48-91-449-46-86

Academic Editor: Gianluca Di Profio

Received: 20 January 2016; Accepted: 23 March 2016; Published: 28 March 2016

**Abstract:** The studies on the resistance to degradation of capillary polypropylene membranes assembled in a membrane crystallizer were performed. The supersaturation state of salt was achieved by evaporation of water from the NaCl saturated solutions using membrane distillation process. A high feed temperature (363 K) was used in order to enhance the degradation effects and to shorten the test times. Salt crystallization was carried out by the application of batch or fluidized bed crystallizer. A significant membrane scaling was observed regardless of the method of realized crystallization. The SEM-EDS, DSC, and FTIR methods were used for investigations of polypropylene degradation. The salt crystallization onto the membrane surface accelerated polypropylene degradation. Due to a polymer degradation, the presence of carbonyl groups on the membranes' surface was identified. Besides the changes in the chemical structure a significant mechanical damage of the membranes, mainly caused by the internal scaling, was also found. As a result, the membranes were severely damaged after 150 h of process operation. A high level of salt rejection was maintained despite damage to the external membrane surface.

**Keywords:** membrane distillation; scaling; crystallization; polymer degradation

## 1. Introduction

In the membrane distillation (MD) process, pure water is separated from salt solutions that leads to the supersaturation state of solutes. As a result, a salt crystallizes on the membrane surface resulting in a decrease of process yield and frequently leads to irreversible damage of the membrane modules [1–3]. This problem can be solved by integration of membrane distillation with a crystallization unit—membrane distillation crystallizer (MDC) [4–8]. In this system, not only water can be produced from brines and other solutions, but also the solutes can be recovered as solids in the crystallizer. The application of MDC was proposed in a treatment technology of wastewater generated during an electroplating process [9].

The MDC process can be utilized in the integrated system of water desalination. However, a limited solubility of salts and increasing osmotic pressure results in fresh water obtained in the reverse osmosis (RO) process being constituted of about 40%–50% volume of desalinated seawater and the remaining RO retentate forms a brine, which is subsequently discharged as a secondary waste stream. This problem can be solved by performing the desalination in a RO-MDC system [5,6,10–12]. In this case, the water is produced from RO retentate in the MD stage and solids salts in the crystallizer, which allows realization of a zero discharge concept of the concentrated brine into the environment [11].

The major operational problem in the MDC system is an appropriate control of supersaturation during the process, which eliminates the nucleation and crystals formation on the membrane surface. A crystallizer design and operating effectiveness can influence the scaling intensity that occurs in the MD module [13–15]. The periodical, cooling crystallizers are often used when temperature has a large

influence on the solubility. Therefore, this method is not useful for NaCl, because temperature has little effect on the solubility in this case [4,5], and evaporative crystallizers are used for crystallization of this salt. A continuous NaCl crystallization can be carried-out using Oslo fluidized-bed crystallizer [16]. In units of this type, a bed of crystals is suspended in the saturated solution. The salt removal by fluidized-bed method was also applied in water desalination processes. The salt removal by seeding in a fluidized-bed crystallizer was found to be a feasible method for the reduction of scaling tendency of seawater [17]. This method is based on introducing seed (salt crystals) of the same type as the scaling materials to the metastable salt solution in order to reduce its supersaturation by heterogeneous crystallization. The fluidized-bed reactor was applied for scaling elimination during water desalination by RO process [18].

In the MD process, hydrophobic membranes are used, the pores of which can be only filled by the gas phase. The formation of deposits on the membrane surface (fouling and scaling) cause the wettability of the surface pores by separated solutions [2–5]. The water evaporation from the crystal surface facilitates the secondary nucleation; therefore, the surface scaling can also develop into internal membrane scaling. The growth of salt crystals in the pores interior may cause the blockage of pores, enhancement of surface roughness, and even mechanical damage of the membrane walls [2,5,13]. With regard to these phenomena, an elimination of crystallization in the MD module is a basic condition for an efficient operation of MDC.

A fulfillment of the above mentioned condition is possible when the applied parameters of MDC operation prevent the formation of a supersaturation state at the membrane surface. This can be achieved by selecting a temperature and the flow rate of feed and distillate through the MD module [5,11]. It is also essential that the residence time of solution in the crystallizer avoids the supersaturation state caused by rapid water evaporation in the MD process [14]. With regard to this, it is advantageous to limit a magnitude of the driving force of mass transfer, which is proposed by using low feed temperature [5,6,8]. Such effect can be also obtained by elevation of distillate temperature, which additionally limits the heat loss by conduction [15]. However, the effectiveness of these solutions requires the selection of operation parameters for a given MDC design. For this reason, it is more advantageous to use a multistage MDC with a continuous operation, in which unsaturated solution is obtained in the final stage (before MD unit) by heating the feed and by adding a fresh portion of unsaturated salt solution into the feed [7,11].

The crystallization of salt on the surface of hydrophobic membranes caused their wettability due to contact of the feed with salt crystals surface. The membrane wettability in the MD process can also be as a result of chemical degradation of polymer, which causes the formation of hydrophilic groups on the membrane surfaces [19]. In the MD process, the membranes from polypropylene are frequently used [7,9]. These membranes exhibit a good thermal and chemical resistance, which allowed to maintain their non-wettability during long-term studies of water desalination [20]. During the studies with concentrated NaCl solutions, it was found that a four-year contact of PP film with the saturated salt solution caused only a slight degradation of polymer [21]. It can be assumed that the conditions existing in the MDC (e.g., elevated temperature and salt crystallization) can cause a larger degradation of PP.

In the presented work, the studies were performed on the resistance to polymer degradation and the wettability of PP membranes used for the separation of supersaturated NaCl solutions. A scaling intensity in the MDC installation can be reduced by using at least a two-stage system: crystallizer-MD installation. However, the salt crystallization may proceed in the MD module even in a multi-stage MDC. In order to accelerate the degradation process, a high feed temperature was used and a single-stage MDC, which facilitates the salt crystallization on the membrane surface [2,6].

## 2. Experimental Section

The membrane degradation usually proceeds very slowly and negative effects of this process are observed after e.g., 1–2 years of MD module exploitation [19–22]. Therefore, a single-stage MDC

installation schematically presented in Figure 1 was used for accelerate the polypropylene degradation phenomenon during a short period of laboratory examination.

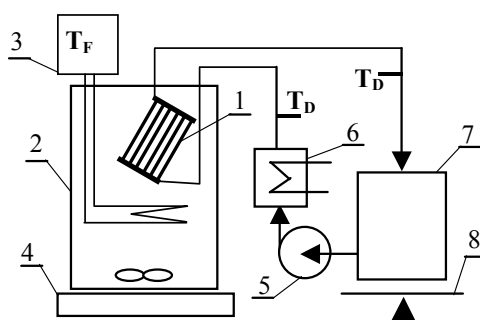


**Figure 1.** Scheme of experimental set-up. 1—MD module; 2—crystallizer; 3—Nüga temperature regulator; 4—magnetic stirrer; 5—peristaltic pump; 6—thermostat; 7—distillate tank; 8—balance.

A submerged MD membrane module (without housing) was assembled inside the upper part of crystallizer in the applied experimental set-up (Figure 1). The studies were performed using alternately one of the modules having a similar design and the external surface of respectively  $0.01 \text{ m}^2$  (MD1) and  $0.0096 \text{ m}^2$  (MD2). In each module, ten capillary polypropylene membranes Accurel PP S6/2 (Membrana GmbH, Wuppertal, Germany) were assembled (Figure 2). The capillary diameters were 1.8/2.6 mm, nominal and maximum diameters of the pores were  $0.2 \text{ }\mu\text{m}$  and  $0.6 \text{ }\mu\text{m}$ , respectively, and the open porosity was 73% (manufacturer's data).

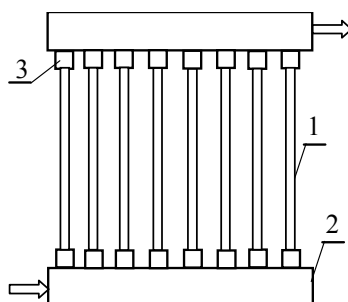


**Figure 2.** The design of used submerged MD module. 1—Accurel PP S6/2 membrane; 2—module head; 3—membrane potting.

A solution temperature inside the crystallizer was fixed at  $363 \pm 1 \text{ K}$  by Nüga temperature regulator (Germany). The distillate ( $323 \text{ K}$ ) flowed inside the capillaries (lumen side), from the bottom to the upper part of the MD module. A peristaltic pump was used to obtain the volume flow velocity of distillate stream equal to  $6 \pm 0.2 \text{ mL/s}$ . At the beginning of each measurement series, the distillate loop was refilled by  $0.5 \text{ L}$  distillate water ( $2\text{--}3 \text{ }\mu\text{S/cm}$ ). The permeate flux was calculated on the basis of changes in the distillate volume over studied period of time.

A diluted NaCl (ChemPur, Piekary Śląskie, Poland) solution ( $10 \text{ g/L}$ ) was used for determination of maximal permeate flux for both modules MD1 and MD2. A solution of  $300 \text{ g NaCl/L}$  was utilized to study a level of flux decline when almost saturated solution fed the MD module.

Seawater contains, besides NaCl, several other ions, and some of them may form sparingly soluble solutes. Therefore, the crystallization studies were carried out using the saturated brine (at room temperature) which was prepared with NaCl crystal salts purchased in a local market. This salt beside NaCl (98.5%) contained several other ions, such as  $\text{SO}_4^{2-}$ ,  $\text{K}^+$ ,  $\text{Ca}^{2+}$ ,  $\text{Si}^{4+}$ , and  $\text{Mg}^{2+}$  (manufacturer's data, Kłodzko Salt Mine, Wieliczka, Poland). The content of crystallizer was agitated using a magnetic stirrer ( $1000 \text{ rpm}$ ).

The salt crystallization was carried out using a batch or fluidized-bed crystallizer. In the first case (MD1 module), a crystallizer was filled with 3 L of brine, then a solution was preheated to 363 K and the MD process was further carried out for about 5 h. After completing the process, the MD1 module was taken out from crystallizer and was then stored in distilled water overnight (Mode I).

In the second case (fluidized-bed crystallizer) the MD2 module was used. The process was performed in the following way: after preheating 3 L of brine to 363 K, about 30–45 g of NaCl crystals (initial 80 h of studies) or 90 g of NaCl (from 80 h of studies) was added to the crystallizer, and finally saturated solution (363 K) with suspension of salt crystals was obtained. An intensive mixed (1000 rpm) suspension of salt crystals created the fluidized bed. Two methods were applied (Mode I and Mode II) for a periodical dissolution of salt crystals from membrane surfaces in MD2 module. Mode I was similar as in the case of MD1 module—after 5 h of process the MD2 module was taken out from crystallizer and was then rinsed with distilled water. In the second variant of process operation (Mode II), the membranes were additionally rinsed with distilled water for about 1 min at every 30 min, which allowed removal of the NaCl crystals from the membrane surface.

The morphology of membrane and the deposit formed during the process was studied using a Jeol JSM 6100 scanning electron microscopy (SEM-EDS). The samples for cross-section observations were prepared by fracturing the capillary membranes in liquid nitrogen. All the samples were sputter coated with gold and palladium. The electrical conductivity of solutions was measured with a 6P Ultrameter (Myron L Company, Carlsbad, CA, USA).

In order to identify the functional groups on the polypropylene surface, the attenuated total reflection Fourier transform infrared (ATR-FTIR) analyses were performed using a Nicolet 380 FT-IR spectrophotometer connected with Smart Orbit diamond ATR accessory (Thermo Electron Corp., Waltham, MA, USA).

The measurements of phase transition temperatures of polymers can be useful indicator for evaluation of the extent of polymer degradation. The thermal properties of used polypropylene membranes were evaluated by differential scanning calorimetry (DSC). The measurements were performed with the use of Q1000 TA Instruments apparatus, at heating-cooling rate of 10 deg/min.

### 3. Results and Discussion

#### 3.1. Batch Crystallizer

A maximum yield of applied design of submerged MD modules was determined using a dilute NaCl solution (10 g NaCl/L) as a feed. The permeate flux at a level of 580–600 L/m<sup>2</sup>·d was achieved for MD1 module (feed temperature 363 K, distillate temperature 323 K). However, the permeate flux decreased to 540 L/m<sup>2</sup>·d during 15 h of module operation (Figure 3). From the previous studies [22] it is a known fact that a fraction of the pores located on the surface of Accurel PP membranes underwent the wettability at the initial period of MD process, resulting in a decline of the permeate flux. A low value of obtained electrical conductivity of distillate in the range of 4–6 μS/cm (feed 10 g NaCl/L), confirms that the membranes underwent only the surface wettability during the first 15 h of studies.

In the second stage of studies, an NaCl solution with initial concentration of 300 g/L was used as a feed to determine of MD efficiency. The presence of salt decreased the driving force (partial pressure difference), and as a result, the permeate flux for almost saturated NaCl solution was decreased from 540 to 150 L/m<sup>2</sup>·d, whereas a value of the electrical conductivity increased to 70 μS/cm (Figure 3). This value of conductivity was increased to 90 μS/cm, and the permeate flux decreased to 110 L/m<sup>2</sup>·d after 40 h of MD1 module exploitation. When brine was exchanged into a dilute NaCl solution, the maximal permeate flux was also significantly decreased during the separation process, from 540 to 480 L/m<sup>2</sup>·d (Figure 3, 44 h). These results indicate that not only the pores on the membrane surface, but also some pores inside the wall underwent the wettability. The wetting of pores may be caused by the crystallization of salt on the membrane surface, which is frequently observed in MDC studies [2,5].

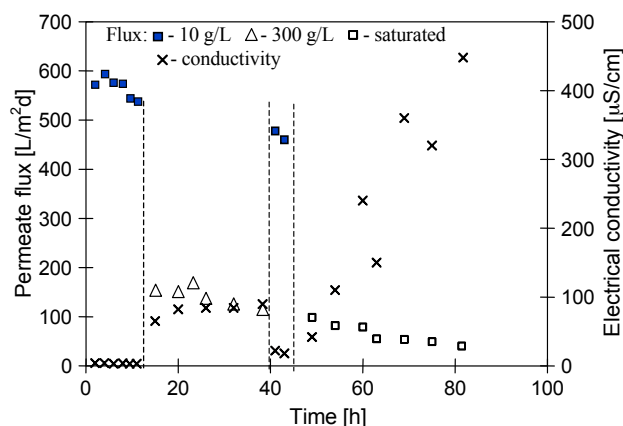


**Figure 3.** Changes of the permeate flux and distillate electrical conductivity during MD of NaCl solutions. Feed initial concentration: 10 g/L, 300 g/L and saturated (at 293 K) solution. Module MD1.

The above phenomenon was confirmed by the results of consecutive measurements of MDC (Figure 3, from 50 h), in which a saturated (at room temperature) NaCl solution was used as a feed. After 2–3 h of MD process, a suspension of an increasing number of salt crystals was observed in the feed. After completing measurements, the presence of salt crystals was also found on the membrane surfaces. The MD1 module was stored overnight in the distilled water, resulting in the dissolution of salt crystals from membrane surfaces. However, the periodical dissolution of salt crystals deposited on the membrane surfaces (probably also inside the pores) caused the electrical conductivity of distillate to systematically increase in the consecutive days, reaching a value of 450  $\mu\text{S}/\text{cm}$  after additional 35 h of crystallizer operation (Figure 3, 83 h). Such a value of electrical conductivity corresponds to a concentration of about 0.2 g NaCl/L, thus a 99.9% of salt retention was maintained. However, taking into account the need of long-term exploitation the MDC system, the obtained results confirmed a conclusion from other works, that one of basic conditions of appropriate operation of MDC is elimination of salt crystallization on the membrane surface [5]. The scaling intensity in the MD1 module was studied using SEM methods, and the results of these observations were presented in Section 3.3.

### 3.2. Fluidized-Bed Crystallizer

A heterogeneous crystallization on the surface of seeding salt crystals is proposed as a method of scaling elimination in the installations for water desalination [17,18]. The effectiveness of such solution was also tested in this work by location of the MD2 module directly inside a fluidized-bed crystallizer. The saturated brine with NaCl crystals was rigorously mixed in order to create the bed of suspended crystals around the membranes in the MD2 module assembled in the upper part of crystallizer (Figure 1). The obtained results of these studies were presented in Figures 4 and 5.

Although the values of maximal permeate flux of the modules MD1 and MD2 were similar (Figures 3 and 6), the permeate flux obtained for MD2 module during MDC studies was at a level of 3–4  $\text{L}/\text{m}^2 \cdot \text{d}$  (Figure 4), which was significantly smaller than the values obtained for MD1 (Figure 3).

It should be remembered, that each point on the figures represents the average permeate flux obtained during 5 h of MD process operation. In the case of results presented in Figure 3 (module MD1), a saturated salt solution (at room temperature) was used as a feed. Due to preheating of the feed to 363 K, this solution became unsaturated at the beginning of measurement and the supersaturation state was achieved after 2–3 h of MD process. A growth of NaCl crystals in the feed was observed after this period. Moreover, the module MD1 was rinsed using distilled water (mode I) after the measurements; therefore, the NaCl crystals located on the membrane surface were dissolved. On the other hand, the operating conditions of MD2 module (solution saturated at 363 K) facilitate a membrane scaling from

the beginning of measurement, which was most probably a reason for lower module yield. The larger scaling observed in the MD2 module was also confirmed by the fact that after 80 h of process duration the distillate conductivity was increased to 1500  $\mu\text{S}/\text{cm}$  (Figure 6), whereas for MD1 module and over a similar period, the value 450  $\mu\text{S}/\text{cm}$  was obtained (Figure 3).

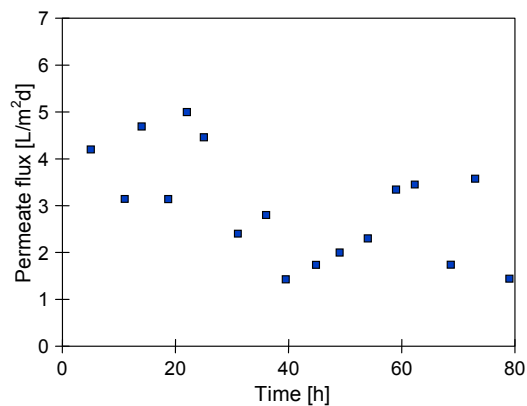


**Figure 4.** Changes of the permeate flux during MD of NaCl saturated (at 363 K) solutions. Module MD2 assembled inside fluidized-bed crystallizer. Mode I.

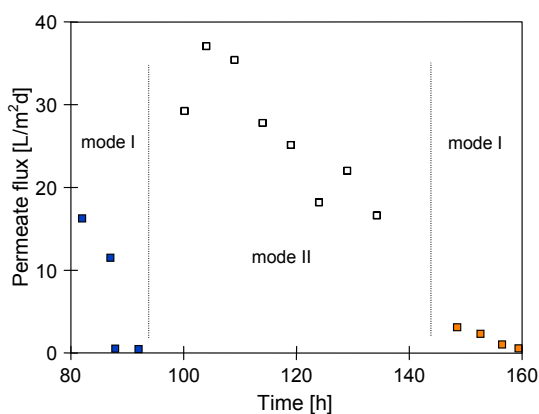


**Figure 5.** Changes of the permeate flux during MD of NaCl saturated (at 363 K) solutions. Module MD2 assembled inside fluidized-bed crystallizer. Mode I—continuous feed concentration, mode II—feed concentration with periodical membrane rinsing with distilled water.

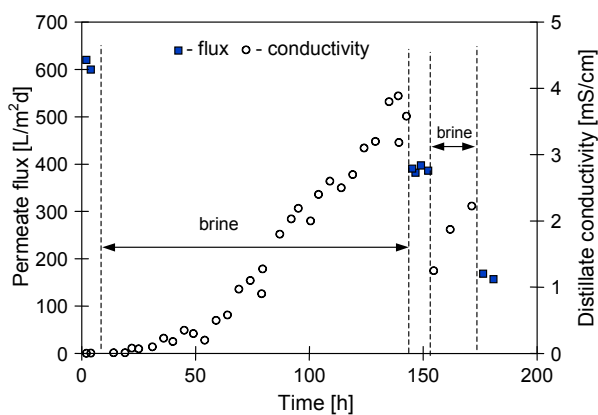


**Figure 6.** Changes of the maximal permeate flux (feed 10 g NaCl/L) and distillate electrical conductivity during MD of NaCl saturated solutions. Module MD2.

It was found, that the permeate flux fluctuation with the time presented in Figure 4, resulted from variations of the amount of salt crystals dosing into the crystallizer. For this reason, the MD2 module was thoroughly rinsed with distilled water after 80 h of studies and further studies were performed dosing a constant amount of salt (30 g/L). As a result, a significantly larger yield of MD process was obtained; however, the permeate flux was quickly decreasing to values close to zero during consecutive measurements (Figure 5). This indicates that despite a substantial increase of the number of suspended crystals, a salt crystallization was not only on their surface, but also on the membranes. A visual inspection of MD2 module revealed that the salt crystals covered all the membrane surfaces, which blocked the pores and significantly reduced the surface for water evaporation.

Negative effects of scaling (pore blockage) were confirmed by the fact that definitely higher values of the permeate flux were achieved when a scaling intensity was limited using a periodical rinsing (every 30 min) of the membranes with distilled water (Figure 5, mode II). However, despite membrane rinsing during the consecutive 50 h of studies, the permeate flux was decreased from 38 to 17 L/m<sup>2</sup>·d. Moreover, a continuous increase of the distillate electrical conductivity was observed during this period (Figure 6). The results presented in Figures 5 and 6 indicate that, performed due to mode II, cyclic repetition of crystals formation on the membrane surfaces and crystals dissolution by water rinsing favors the pore wetting. Pore wetting is confirmed also by the fact that, as a result of brine separation, a maximal permeate flux determined for MD2 module after 150 h of exploitation decreased from 600 to 400 L/m<sup>2</sup>·h (Figure 6). However, the MD2 module still maintained a high salt rejection amounting to over 99% for saturated NaCl solution, despite the increase of distillate conductivity to 4000 µS/cm.

During the last 15 h of MD2 module operation, the studies of MDC without the periodical rinsing of the membranes with distilled water were again conducted (Figure 5, mode I—from 144 h). A further crystallization of salt on the membrane surface caused a decline of maximal permeate flux from 400 to 150 L/m<sup>2</sup>·d (Figure 6). Moreover, a rapid deterioration of mechanical properties of the membranes was also observed over this period. The membranes became brittle, and fragments of polymer were detached from their external surface.

### 3.3. SEM Observations

After completing the MDC studies, the membrane samples were collected from modules MD1 and MD2 for SEM observations. The surfaces of membranes removed from the crystallizer were rinsed with distilled water and the samples were subsequently dried in a natural way at ambient temperature. The SEM observations revealed that, during the MDC studies, the membrane surface was significantly changed in a comparison to an image of a new membrane presented in Figure 7.

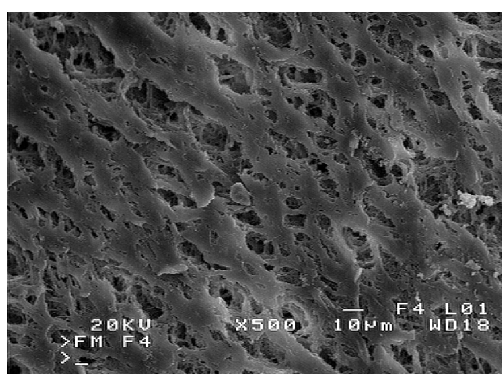


**Figure 7.** SEM image of the external surface of new Accurel PP S6/2 membrane.

In accordance with predictions, the smallest changes were observed in the case of the membranes from MD1 module. The presence of many clusters of fine deposits was found on the membrane surface,

but the surface pores were not completely covered by deposit (Figure 8). The SEM-EDS analysis of deposits revealed that they were mainly composed of Na, Cl, and Si, and in a smaller amount from Ca, Mg, and P.

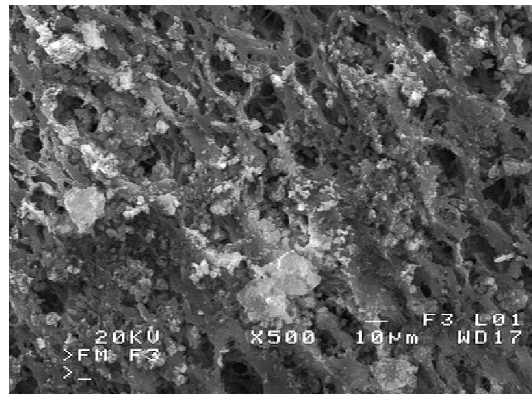


**Figure 8.** SEM image of salt deposits on the membrane surface. Module MD1.

A similar composition had a deposit formed on the membrane surface in the module MD2. However, a deposit layer was thicker and, in this case, covered the majority of the surface pores (Figure 9A). The formed deposit also fulfilled the pores inside the membrane wall at the depth up to almost 100  $\mu\text{m}$  (Figure 9B). The internal scaling was one of main reasons for such a significant reduction of module efficiency (Figures 5 and 6). Moreover, the salt crystallization caused the polymer fragments to detach from the membrane walls (Figure 10). A boundary between the external membrane surface (bottom of figure) and a damaged fragment of the membrane wall was shown in Figure 11A. Due to detachment of the external surface from capillary, the pores inside the wall were exposed, and a magnification view of these pores was presented in Figure 11B. The SEM-EDS analysis revealed, that the structure indicated by arrow on area “SD” is inorganic deposit, which crystallized inside the membrane wall. The same deposits occurred numerously in the other places of the damaged wall (lighter points at top of Figure 11A). The salt crystals growing inside the membrane most probably caused a detachment of membrane fragments. The changes of the structural and chemical properties of polypropylene membranes caused by the salt crystallization were also found in other work [23]. A partial wettability due to a salt crystallization of used Accurel PP S6/2 was observed in work [24]. Moreover, it was also demonstrated in this work, that enhancement of hydrophobicity of PP membranes limited the penetration of salt into the membrane pores.

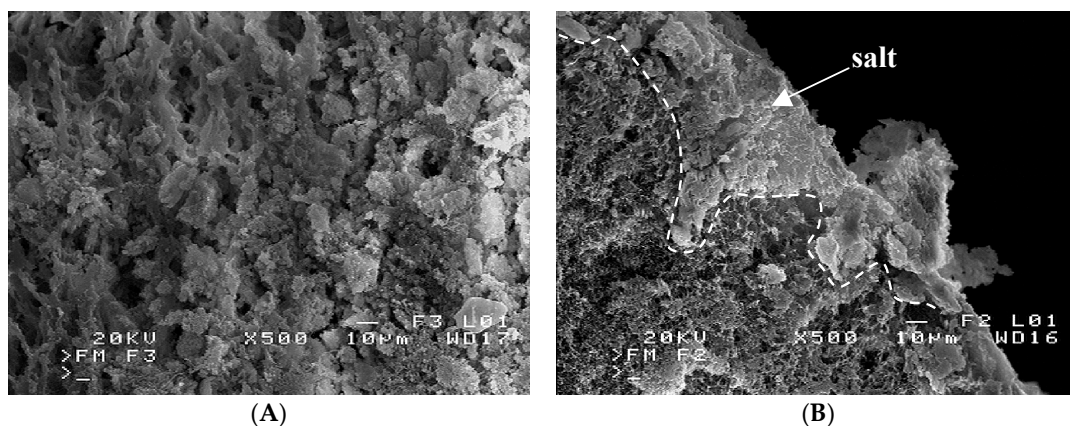


**Figure 9.** SEM images of salt deposits on: (A) membrane surface; (B) inside the membrane wall. Module MD2.

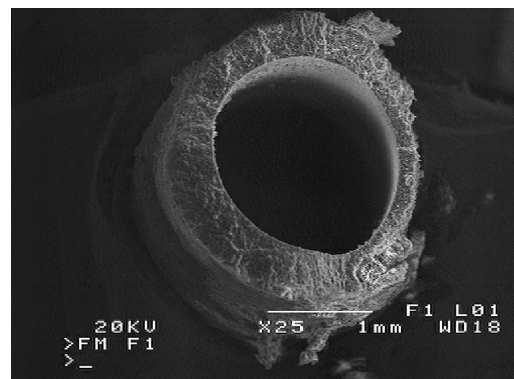


**Figure 10.** SEM image of membrane cross-section. Membrane sample from MD2 module.

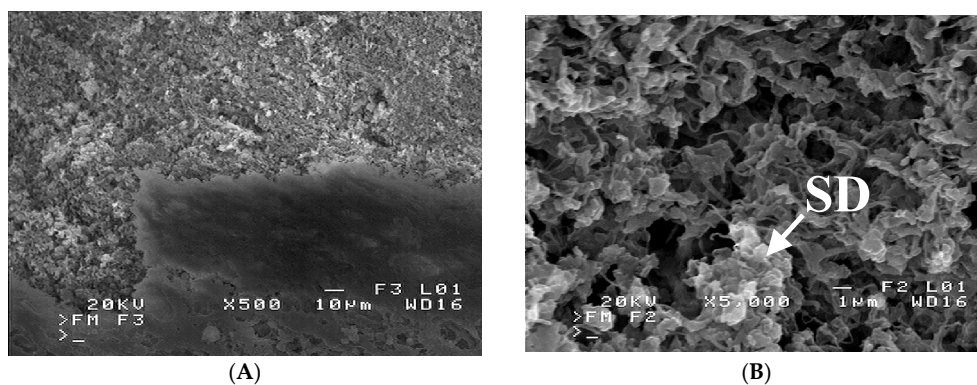


**Figure 11.** SEM images of membrane external surface: (A) a part of wall was detached (top of figure); (B) detached wall with salt deposit (SD). Module MD2.

The salt crystals were also observed in many places on the membrane surface on the lumen side (Figure 12). The distillate flows inside the lumen side, which excludes the salt crystallization during MD process. However, the electrical conductivity of distillate was increased to  $4000 \mu\text{S}/\text{cm}$  (Figure 6) which indicates a slight feed leakage through wetted fragments of the membrane wall. After completing the studies, the membranes were dried. The hydrophobic properties of PP caused, that a NaCl solution was pushed out from the pores interior on the membrane surface, where it evaporated and as a result, the salt crystals were formed. Thus, it can be concluded, that the NaCl crystals formed on the membrane surface on the distillate side indicate the places in which the membrane walls were wetted.

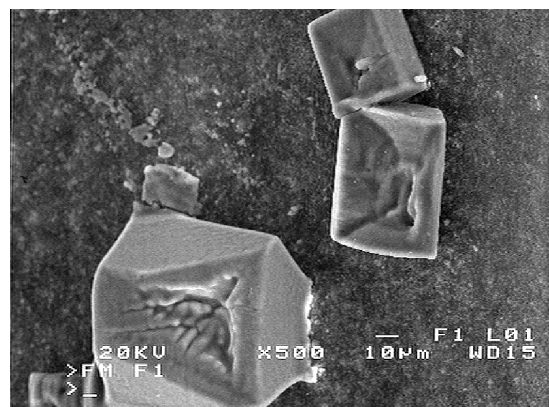


**Figure 12.** SEM images of salt crystals formed on the distillate side during membrane drying.

### 3.4. Membrane Degradation

New capillary Accurel PP membranes are flexible, and they may be bent without causing damages. However, the membranes used in the MD1 module become rigid; therefore, the walls collapsed when the capillaries were bent. The membranes underwent degradation in the highest degree in the MD2 module. In this case, a slight bending of the membranes caused their fracture. Moreover, the wall fragments were detached from the membrane surface (Figure 10), and these fragments can be easily ground into a powder. Such a state of the membranes material indicates that a significant degradation of polypropylene proceeded during the studies of MDC process.

Polypropylene is a semicrystalline polymer and its mechanical properties depend to a large degree on a ratio of the crystalline phase to amorphous phase [19]. A consequence of polymer degradation is a change of the crystallinity degree of PP and a change in the chemical composition [19,21,24]. The FTIR and DSC analyses were performed in order to determine the intensity of these changes.

The polypropylene FTIR spectrum had a characteristic methyl absorption band at  $1375\text{ cm}^{-1}$ , and doublet at  $1167$  and  $973\text{ cm}^{-1}$  [25]. The bands that can be used to determine the crystallinity of PP appeared at  $1167$ ,  $997$  and  $841\text{ cm}^{-1}$ , and moreover, bands at  $1219$ ,  $1167$ ,  $997$ ,  $972$ ,  $899$  and  $841\text{ cm}^{-1}$  are characteristic for isotactic PP [25,26]. A comparison of FTIR spectra obtained for new Accurel PP S6/2 membrane and samples collected from MD1 and MD2 modules was presented in Figure 13, and the FTIR spectra magnified in the region  $400\text{--}1900\text{ cm}^{-1}$  was shown in Figure 14. The essential changes either in the shift or new bonds were not observed. Only a low intensity band was observed in the region of  $1700\text{--}1750\text{ cm}^{-1}$ , which can indicate that the carbonyl groups were created [25]. This is a weak band and was also observed for Accurel PP membranes soaked in hot distilled water [19]. The obtained results indicate that the applied PP membranes demonstrated a good chemical resistance during the MDC studies. For this reason, the observed membrane degradation was not caused by the changes in the chemical composition of polymer. However, the results presented in Figures 13 and 14 demonstrated that a significant decrease of intensity of characteristic bands for crystallinity/isotacticity of iPP structure was observed in the spectra of samples collected from MD modules. This confirms a fact, that the changes in the polymer structure (crystallinity) were the main reason of increase of membrane embitterment during the MDC studies.

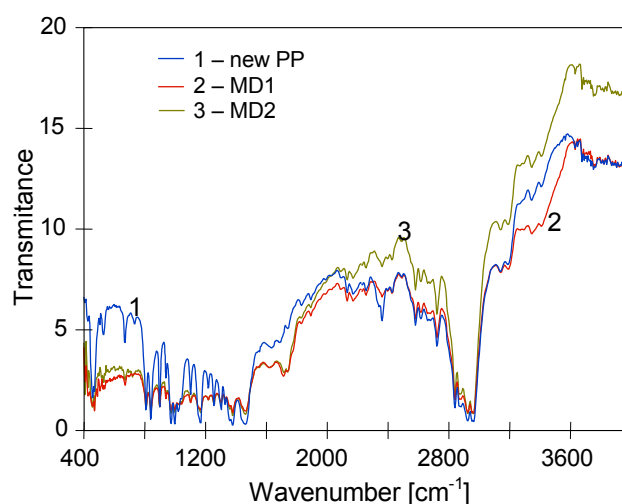


**Figure 13.** Comparison of FTIR spectra recorded for new Accurel PP S6/2 membrane and for membrane samples removed from MD1 and MD2 modules.

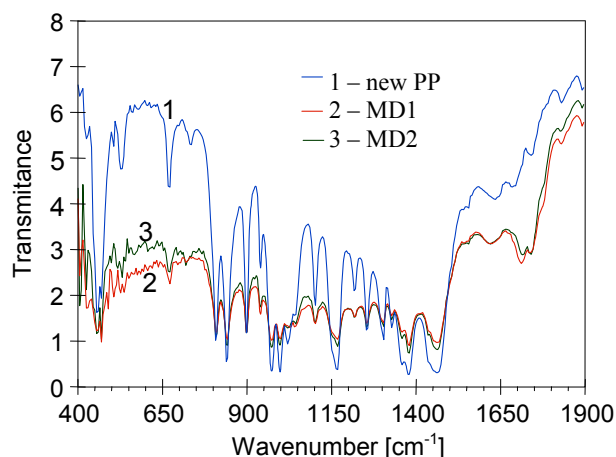


**Figure 14.** Comparison of FTIR spectra recorded for new Accurel PP S6/2 membrane and for membrane samples removed from MD1 and MD2 modules.

Although the membranes in the MD2 module underwent a significantly larger degradation, only small differences in the peaks intensity were observed for samples collected from MD1 and MD2 modules (Figures 13 and 14). Thus, it can be concluded that a high feed temperature was the main reason of variations in the crystallinity degree of PP [26]. Moreover, an internal scaling caused a larger degradation of the membranes in the MD2 module.

The changes in the polymer matrix were also confirmed by the results of DSC studies presented in Figure 15 and Table 1. The melting ( $T_m$ ) and crystallization ( $T_C$ ) temperatures were determined from both the first and the second scans. A decrease of  $T_m$  and melting enthalpy ( $\Delta H_m$ ) was found for membranes after salt crystallization studies. A decrease of melting enthalpy was also observed in the second heating. A decrease of  $\Delta H_m^{\text{II}}$  values indicated that the polymer crystallinity was reduced. The melting heat was used to determine the percent crystallinity using the reference value for polypropylene  $\Delta H_{m,100\%} = 207 \text{ J/g}$  [27]. The new polypropylene membranes were characterized by a value of crystallinity degree at a level of 41.2%, and decreased to 39.2% for membranes from the MD2 module. These results confirm a fact that the degree of PP degradation increases along with the exploitation time of the MD module.

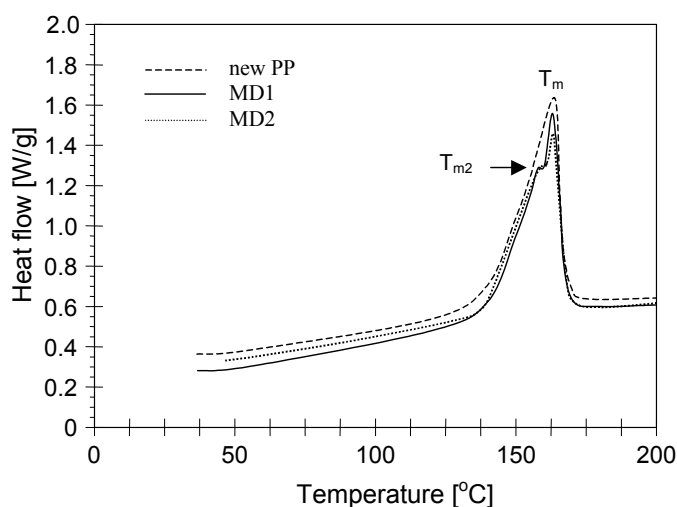


**Figure 15.** DSC heating curves (I scanning) of new Accurel PP S6/2 membrane and membrane samples removed from MD1 and MD2 modules.

**Table 1.** The results of DSC analysis. MD2 cleaned—the external (degraded) layer of membrane was removed.

Sample	I Scan (Heating)			Cooling (Crystallization)		II Scan (Heating)		
	$T_m$ (°C)	$T_{m2}$ (°C)	$\Delta H_m$ (J/g)	$T_c$ (°C)	$\Delta H_c$ (J/g)	$T_m^{II}$ (°C)	$\Delta H_m^{II}$ (J/g)	Crystallinity (%)
New PP	164.6	- *	88.6	117.9	88.8	161.8	86.9	41.9
MD	163.9	157.9	85.9	117.8	88.1	160.5	85.1	41.1
MD1	163.3	158.3	84.3	117.6	84.7	160.4	82.4	39.8
MD2	162.9	157.3	81.4	116.9	81.6	160.2	81.2	39.2
MD2 cleaned	164.2	- *	80.1	117.4	89.9	161.2	84.4	40.8

Notes:  $T_m$ ,  $T_c$ —melting and crystallization temperatures;  $\Delta H_m$ ,  $\Delta H_c$ —melting and crystallization enthalpy.  
\*—formation of the second melting peak on a lower-temperature shoulder of the main transition was observed.

The formation of the second melting peak was observed during the first heating of samples collected from MD modules (Figure 15,  $T_{m2}$ ). The  $T_{m2}$  values were lower than that of  $T_m$ , which indicates that the secondary structure with definitely shorter polymer chains was formed in the polymer matrix. The lowest value of  $T_{m2} = 157.3$  °C was achieved for membranes from the MD2 module, which exhibited the largest mechanical damage. In this case, almost half the thickness of wall (Figure 10) was changed into fracturing layer, easy to scraps. After the removal of this layer, the performed DSC analysis demonstrated, that such prepared membrane (Table 1, MD2 cleaned) had the parameters closed to those obtained for a new membrane. A layer of the wall, which was detached from the external membrane surface, was subjected to high feed temperature (363 K) during MDC studies and the internal scaling proceeded inside this layer (Figure 9B), which probably accelerated cracking of the polymer chains due to the synergistic effect. This conclusion is confirmed by the results presented in [28]. In this work, the same Accurel PP S6/2 membranes were used (over 180 h) for separation of feed contained 250 g NaCl/L at temperature 363 K. The DSC analysis (Table 1, sample MD) indicated that such high feed temperature caused changes in the polymer parameters, but smaller than that observed for samples from MD1 and MD2 modules. Moreover, the salt crystals were not created (feed 250 g NaCl/L) during this study, and beside high feed temperature after 180 h of MD process duration the membranes were still flexible. Thus, a limitation of salt crystallization on the membrane surface significantly reduces the degree of membrane degradation in spite of high feed temperature.

#### 4. Conclusions

The separation of salt solutions in MD process at a temperature of 363 K and the occurrence of intensive scaling caused a fast degradation of used capillary polypropylene membrane. As a result, a fracture of the membrane wall after 150 h of module exploitation was observed. Such performance restricted the practical implementation of MDC process in a single stage, even with a periodical removal of crystallized salt from the membrane surface. An attempt to reduce the scaling potential by application of heterogeneous crystallization on the surface of seeding salt crystals inside fluidized bed crystallizer was also inefficient.

As a result of PP degradation during the MDC studies, more than half the thickness of the membrane wall was destroyed. Despite such significant damage, the used membranes still maintained their nonwettability and the degree of salt separation exceeding 99% was retained. Such a result confirms the conclusions from previous works indicating the suitability of PP membranes for the MD process.

A limitation of salt crystallization on the membrane surface significantly reduces the degree of membrane degradation in spite of high feed temperature. This indicates that the application of

multi-stage systems eliminating the creation of supersaturated state inside the MD module will enable enhancement of the MDC productivity by the application of higher feed temperature.

The PP membranes, in a contact with hot (363 K) saturated NaCl solution maintained their good resistance to the chemical transformation. The formation of carbonyl groups on the membrane surface was only found.

**Acknowledgments:** The National Science Centre Poland is acknowledged for the support of this work (DEC-2014/15/B/ST8/00045).

**Conflicts of Interest:** The authors declare no conflict of interest.

## References

1. Adham, S.; Hussain, A.; Matar, J.M.; Dores, R.; Janson, A. Application of membrane distillation for desalting brines from thermal desalination plants. *Desalination* **2013**, *314*, 101–108. [[CrossRef](#)]
2. Gryta, M. Calcium sulphate scaling in membrane distillation process. *Chem. Pap.* **2009**, *63*, 146–151. [[CrossRef](#)]
3. Ji, Z.; Wang, J.; Yin, Z.; Hou, D.; Luan, Z. Effect of microwave irradiation on typical inorganic salts crystallization in membrane distillation process. *J. Membr. Sci.* **2014**, *455*, 24–30. [[CrossRef](#)]
4. Edwie, F.; Chung, T.S. Development of hollow fiber membranes for water and salt recovery from highly concentrated brine via direct contact membrane distillation and crystallization. *J. Membr. Sci.* **2012**, *421–422*, 111–123. [[CrossRef](#)]
5. Edwie, F.; Chung, T.S. Development of simultaneous membrane distillation-crystallization (SMDC) technology for treatment of saturated brine. *Chem. Eng. Sci.* **2013**, *98*, 160–172. [[CrossRef](#)]
6. Tun, C.M.; Fane, A.G.; Matheickal, J.T.; Sheikholeslami, R. Membrane distillation crystallization of concentrated salts-flux and crystal formation. *J. Membr. Sci.* **2005**, *257*, 144–155. [[CrossRef](#)]
7. Gryta, M. Concentration of NaCl solution by membrane distillation integrated with crystallization. *Sep. Sci. Technol.* **2002**, *37*, 3535–3558. [[CrossRef](#)]
8. Curcio, E.; Criscuoli, A.; Drioli, E. Membrane crystallizers. *Ind. Eng. Chem. Res.* **2001**, *40*, 2679–2684. [[CrossRef](#)]
9. Tomaszewska, M.; Gryta, M.; Morawski, A.W. Recovery of hydrochloric acid from metal pickling solutions by membrane distillation. *Sep. Purif. Technol.* **2001**, *22–23*, 591–600. [[CrossRef](#)]
10. Ji, X.; Curcio, E.; Al Obaidani, S.; Di Profio, G.; Fontananova, E.; Drioli, E. Membrane distillation-crystallization of seawater reverse osmosis brines. *Sep. Purif. Technol.* **2010**, *71*, 76–82. [[CrossRef](#)]
11. Chen, G.; Lu, Y.; Krantz, W.B.; Wang, R.; Fane, A.G. Optimization of operating conditions for a continuous membrane distillation crystallization process with zero salty water discharge. *J. Membr. Sci.* **2014**, *450*, 1–11. [[CrossRef](#)]
12. Martinetti, C.R.; Childress, A.E.; Cath, T.Y. High recovery of concentrated RO brines using forward osmosis and membrane distillation. *J. Membr. Sci.* **2009**, *331*, 31–39. [[CrossRef](#)]
13. Tijing, L.D.; Woo, Y.C.; Choi, J.S.; Lee, S.; Kim, S.H.; Shon, H.K. Fouling and its control in membrane distillation—A review. *J. Membr. Sci.* **2015**, *475*, 215–244. [[CrossRef](#)]
14. Gryta, M. Scaling diminution by heterogeneous crystallization in a filtration element integrated with membrane distillation module. *Pol. J. Chem. Tech.* **2009**, *11*, 60–65. [[CrossRef](#)]
15. Gryta, M. Direct contact membrane distillation with crystallization applied to NaCl solutions. *Chem. Pap.* **2002**, *56*, 14–19.
16. Ruthven, D.M. *Encyclopedia of Separation Technology*; Wiley: New York, NY, USA, 1997; Volume 1.
17. Omar, W.; Chen, J.; Ulrich, J. Reduction of seawater scale forming potential using the fluidized bed crystallization technology. *Desalination* **2010**, *250*, 95–100. [[CrossRef](#)]
18. Rahardianto, A.; Gao, J.; Gabelich, C.J.; Williams, M.D.; Cohen, Y. High recovery membrane desalting of low-salinity brackish water: Integration of accelerated precipitation softening with membrane RO. *J. Membr. Sci.* **2007**, *289*, 123–137. [[CrossRef](#)]
19. Gryta, M.; Grzechulska-Damszel, J.; Markowska, A.; Karakulski, K. The influence of polypropylene degradation on the membrane wettability during membrane distillation. *J. Membr. Sci.* **2009**, *326*, 493–502. [[CrossRef](#)]

20. Gryta, M. Long-term performance of membrane distillation process. *J. Membr. Sci.* **2005**, *265*, 153–159. [[CrossRef](#)]
21. Gryta, M. Study of NaCl permeability through a non-porous polypropylene film. *J. Membr. Sci.* **2016**, *504*, 66–74. [[CrossRef](#)]
22. Gryta, M. Wettability of polypropylene capillary membranes during the membrane distillation process. *Chem. Pap.* **2012**, *66*, 92–98. [[CrossRef](#)]
23. Hughes, P.; Fujita, S.; Suye, S.I. A holistic approach into the impact of sodium hypochlorite on polypropylene fibre reinforced concrete. *Constr. Build. Mater.* **2015**, *85*, 175–181. [[CrossRef](#)]
24. Meng, S.; Ye, Y.; Mansouri, J.; Chen, V. Crystallization behavior of salts during membrane distillation with hydrophobic and superhydrophobic capillary membranes. *J. Membr. Sci.* **2015**, *473*, 165–176. [[CrossRef](#)]
25. Scheirs, J. *Compositional and Failure Analysis of Polymers*; Wiley: Chichester, UK, 2000.
26. He, P.; Xiao, Y.; Zhang, P.; Xing, Ch.; Zhu, N.; Zhu, X.; Yan, D. Thermal degradation of syndiotactic polypropylene and the influence of stereoregularity on the thermal degradation behaviour by *in situ* FTIR spectroscopy. *Polym. Degrad. Stab.* **2005**, *88*, 473–479. [[CrossRef](#)]
27. Van Krevelen, D.W. *Properties of Polymers*; Elsevier: Amsterdam, The Netherlands, 1990.
28. El Fray, M.; Gryta, M. Environmental fracture of polypropylene membranes used in membrane distillation process. *Polimery* **2008**, *53*, 865–870.



© 2016 by the author; licensee MDPI, Basel, Switzerland. This article is an open access article distributed under the terms and conditions of the Creative Commons by Attribution (CC-BY) license (<http://creativecommons.org/licenses/by/4.0/>).